Canadian Chemical Transactions Year 2016 | Volume 4 | Issue 1 | Page 77-89

Research Article

DOI:10.13179/canchemtrans.2016.04.01.0258

Kinetics of Solar Light Assisted Degradation of Direct Red 23 on Activated Carbon-loaded Zinc Oxide and Influence of Operational Parameters

Narayanasamy Sobana[1], Kuppulingam Thirumalai[1] and Meenakshisundaram Swaminathan*[1]

[1]*Department of Chemistry, Annamalai University, Annamalainagar – 608 002, India*
[2]*Nanomaterials Laboratory, International Research Centre, Kalasalingam University, Krishnan koil-626126, India.*

**Corresponding Author, Email: chemres50@gmail.com*

Received: *November 25, 2015* ***Revised:*** *January 27, 2016* ***Accepted:*** *January 29, 2016* ***Published:*** *January 30, 2016*

Abstract: The photocatalytic degradation of an azo dye Direct Red 23 (DR 23) with Activated Carbon loaded ZnO (AC-ZnO) as a photocatalyst has been investigated under solar light irradiation. The effects of operational parameters such as pH of the solution, amount of catalyst, initial dye concentration and effect of grinding on photodegradation of DR 23 by ACSD loaded ZnO were analyzed.The degradation of DR 23 follows pseudo-first order kinetics according to the Langmuir-Hinshelwood model. Synergetic effect of AC-ZnO is revealed by its synergetic factor of 1.78. The AC-ZnO shows higher dye degradation efficiency under solar radiation than UV light.

Keywords: Direct Red 23, solar light, degradation, Photocatalyst, Activated carbon, ZnO

1. INTRODUCTION

Due to industrialization, population growth, and urbanization, large amount of waste water has been produced, and in most cases has become a serious environmental problem in many countries. As an ideal green technology, Advanced Oxidation Processes have attracted continuous interest for its potential applications in environmental remediation [1-3]. Among the Advanced Oxidation Processes, semiconductor photocatalysis plays a vital role in the degradation of toxic chemicals using solar light. Owing to the good photoelectric conversion properties and rapid photoresponse, ZnO exhibits high photocatalytic efficiency on decomposing organic pollutants in water. ZnO is an important wide band gap semiconductor material, which has been widely used in catalysis, ceramics, sensors, and optoelectronic devices, due to its excellent optical, peizoelectrical, and magnetic properties. Additionally, ZnO is nontoxic, abundant in reserves, and easy to obtain, which make it an ideal candidate for practical applications [4-10]. Several authors have proposed a number of modifications on the photocatalysts using a variety of supporting materials and by coating methods [11-13]. Development of core/shell structured

materials by adding support material on a nanometer scale has been receiving extensive attention [12, 13].The shell can alter the charge, functionality, and reactivity of surface, or improve the stability and dispersive ability of the core material. Furthermore, catalytic, optical, or magnetic functions can be imparted to the core particles by the shell material. In general, the synthesis of core/shell structured material has the goal of obtaining a new composite material having synergetic or complementary behaviours between the core and shell materials. The core support materials used are silica, alumina, zeolites, clay and activated carbon. They can act as a sink to collect photogenerated electrons from the conduction band of the semiconductor and thus reducing the recombination of photogenerated electrons and holes through increasing the charge separation [14]. Among these materials, activated carbon is the most commonly used adsorbent for water treatment. Activated carbon has a large specific surface area and a well-developed porous structure, resulting in an attractive force toward organic molecules [15–19]. Synergistic effect of the Activated carbon modifies the ZnO particle properties and consequently its photocatalytic behavior [20, 21].

In our earlier work [22, 23] we had reported the preparation of four activated carbon loaded ZnO catalysts with 4, 9, 13 and 23% of AC by weight. Among the four activated carbon loaded catalysts, 9AC–ZnO (9% of AC by weight) had been found to be the most efficient for degradation study and its characterisation had been discussed in detail[23]. In the present work we report the synergetic effect of the catalyst and the optimum parameters for photocatalytic degradation of DR 23 with 9AC–ZnO using solar light.

2. EXPERIMENTAL

2.1. Materials

Direct Red 23 (DR 23), (C.I. No. 29160, molecular formula = $C_{35}H_{25}N_7Na_2O_{10}S_2$, molecular weight = 813.74) was obtained from s.d. fine chemicals. The dye structure is given below. The photocatalyst ZnO was purchased from E. Merck (99% purity). ZnO has a particle size of 0.1– 4 µm with a surface area of 5 m^2 g^{-1}. AC-ZnO catalysts were prepared by a procedure reported from our laboratory [22, 23]. Activated carbons were obtained from three different sources as (i) commercially available activated carbon from SD fine chemicals (ACSD), (ii) activated carbon from treated fly ash residue (ACTFR) and (iii) activated carbon obtained from Palmnut shell by the acid method (ACPNSC). In our study ACSD was found to be most efficient [23,24]. Double distilled water was used to prepare experimental solutions. The pH of the solutions was adjusted using H_2SO_4 or NaOH.

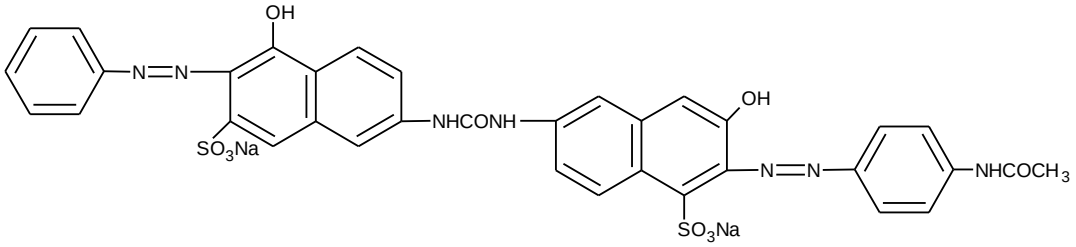

Chemical structure of Direct Red 23

2.2. Irradiation procedure

All photocatalytic experiments were carried out under similar conditions on sunny days between 11 am and 2 pm by reported procedure [25]. An open borosilicate glass tube of 50 mL capacity, 40 cm height and 12.6 mm diameter was used as the reaction vessel. Fifty milliliters of DR 23 ($2x10^{-4}$ M) with the appropriate amount of catalyst was irradiated in the open air and continuously aerated by a pump to provide oxygen and for the complete mixing of reaction solution. A time lag of 30 min was provided prior to illumination to ensure pre-adsorption of the dye on the catalyst. During the illumination time no volatility of the solvent was observed. At specific time intervals, 2-3 mL of the sample was withdrawn and centrifuged to separate the catalyst. One millilitre of the sample was suitably diluted and the absorbance at 242 and 501 nm were measured. The absorbance at 501 nm represents the color of the dye and its decrease indicates decolorization of the dye, whereas the absorption at 242 nm represents the aromatic part of DR 23 and its decrease indicates the degradation of dye. Solar light intensity was measured using LT Lutron LX-10/A digital Lux meter for every 30 min and the average light intensity over the duration of each experiment was calculated. The solar intensity (1250 x100 ±100 lx) was nearly constant during the experiments.

UV spectral measurements were done with Hitachi-U- 2001 spectrometer. The pH of the solution was measured using an ELICO LI-10.

3. RESULTS AND DISCUSSION

3.1 Characteristics of catalyst

AC-ZnO photocatalyst used in this study had been characterized by various surface analytical techniques [23]. XRD analysis of these catalysts shows well crystalline hexagonal phase of ZnO and a small peak at $2\theta = 44.61$ corresponding to AC. BET surface analysis reveal that the surface area of the catalysts increases with the increase in the percentage of AC content . The pore specific volume of AC-ZnO is less when compared to activated carbon, because ZnO particles occupy the pores of activated carbon. AC content of catalysts is increased, the pore specific volume also increases, and it favours higher photocatalytic activity. The DRS results show the increment of surfacial electric charge of oxides by the addition of AC and give an absorption increment in the visible region with a color change from white to blue. From the IR studies [23] we can conclude dye molecules, adsorbed on AC are being transferred to the ZnO present in the pores of the catalyst, where they are degraded on irradiation. SEM images [23] reveal a porous, sponge like structure of the catalyst. It is found that in 9AC-ZnO the AC particles are homogeneously covered by ZnO particles.

3.2. Photodegradability of DR 23

Solar photocatalytic degradation of DR 23 for an initial dye concentration of $2x10^{-4}$ M (163 ppm) with ZnO and 9AC-ZnO is shown in Fig. 1.

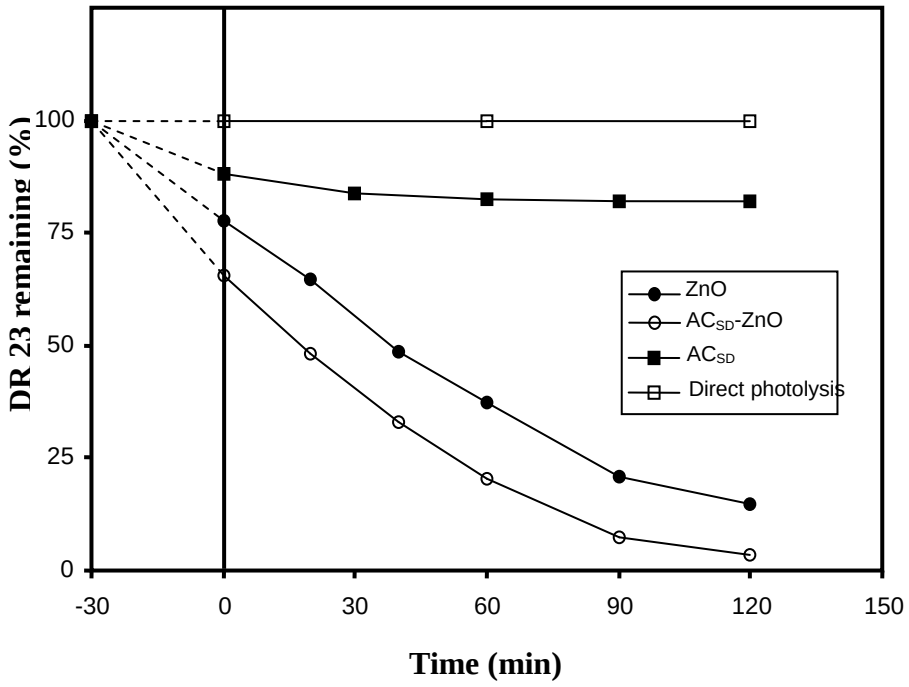

Figure 1. DR 23 degradation in the presence of ZnO, AC_{SD}-ZnO, AC_{SD} using Solar light. C_{SD}-ZnO = 4 g/L, [DR 23] = 2×10^{-4} mol/L, pH = 7.0 ± 0.1

There is no change in concentration of DR 23 when the irradiation was carried out in the absence of catalysts. About 95% of degradation takes place with AC-ZnO at 120 min. Under the same conditions bare ZnO takes 170 min. for complete degradation. This reveals that AC-ZnO is more efficient than bare ZnO for the degradation of DR 23 in solar light. The association of ACSD to ZnO enhances the DR 23 degradation efficiency of ZnO. The photocatalytic degradation of DR 23 dye containing ACSD-ZnO obeys pseudo first order kinetics. At low initial dye concentration, the rate expression is given by

$$d[C]/dt = k'C \qquad \text{---------- (1)}$$

where k' is the pseudo-first order rate constant. The dye is adsorbed onto the AC-ZnO surface and the adsorption–desorption equilibrium is reached. After adsorption, the equilibrium concentration of the dye solution is determined and it is taken as the initial dye concentration for kinetic analysis. Integration of Eq. (1) (with the limit of $C = C_0$ at $t = 0$ with C_0 being the equilibrium concentration of the bulk solution) gives Eq. (2),

$$\ln(C_0/C) = k't \qquad \text{---------- (2)}$$

where C_0 is the equilibrium concentration of dye and C is the concentration at time t. The kinetic curves for ZnO, ACSD-ZnO are of apparent first order as confirmed by the correlation coefficients close to 0.99, obtained from the linear transform $\ln(C_0/C) = k'(t)$ (fig.2).

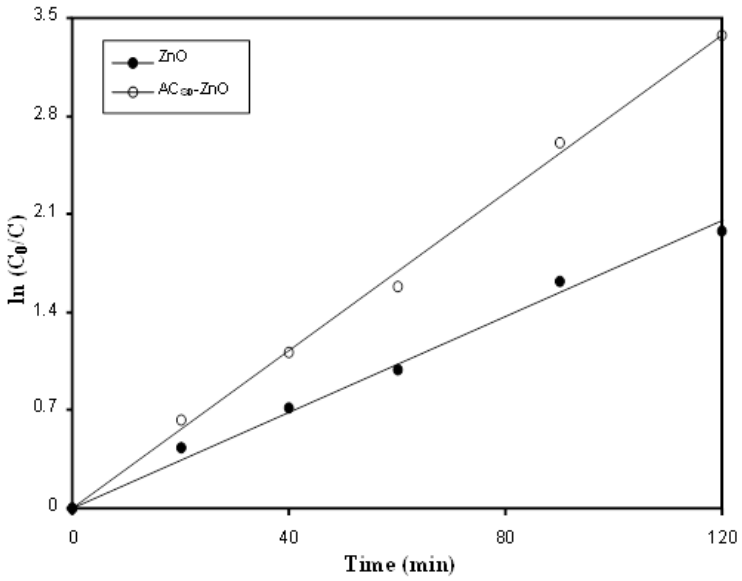

Figure 2. Apparent first-order linear transform ln (C_0/C) = f(t) of DR 23 degradation for ZnO and AC_{SD}-ZnO using Solar light

The strong synergy effect of ACSD is shown by the synergy factor (R) of 1.78 determined by the following equation[22]

$$R = k_{app}\ (AC\text{-}ZnO)/k_{app}\ (ZnO)$$

This reveals that the dye molecules adsorbed in dark are transferred back to solution during irradiation for complete degradation.

3.3. Effect of operational parameters

3.3.1. Effect of catalyst loading

The effect of catalyst weight on the percentage removal of DR 23 was investigated from 1 to 5 g/L of the catalyst. (Fig.3)

Addition of catalyst from 1 to 4 g/L increases the percentage removal of DR 23 sharply. But above 4 g/L of the catalyst, there is no significant increase in decolourisation and degradation efficiencies.The improvement of the removal rate is caused by (i) the increase in the amount of catalyst weight which increases the number of dye molecules adsorbed and (ii) the increase in the density of particles in the area of illumination. At higher concentration of the catalyst (above 4 g L^{-1}), increase is not much because of the light scattering effect by catalyst particles [25]. Hence 4 g/L was used as the optimum catalyst dosage for the solar photocatalytic reactions.

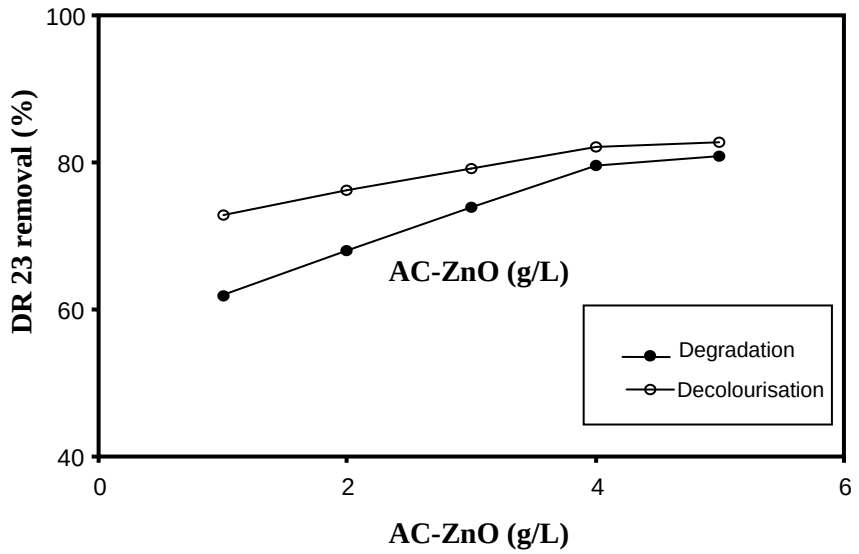

Figure 3. Effect of catalyst loading on the decolourisation and degradation of DR 23 using Solar light. [DR 23] = 2×10^{-4} mol/L, pH = 7.0 ± 0.1, irradiation time - decolourisation = 40 minutes, degradation = 60 minutes.

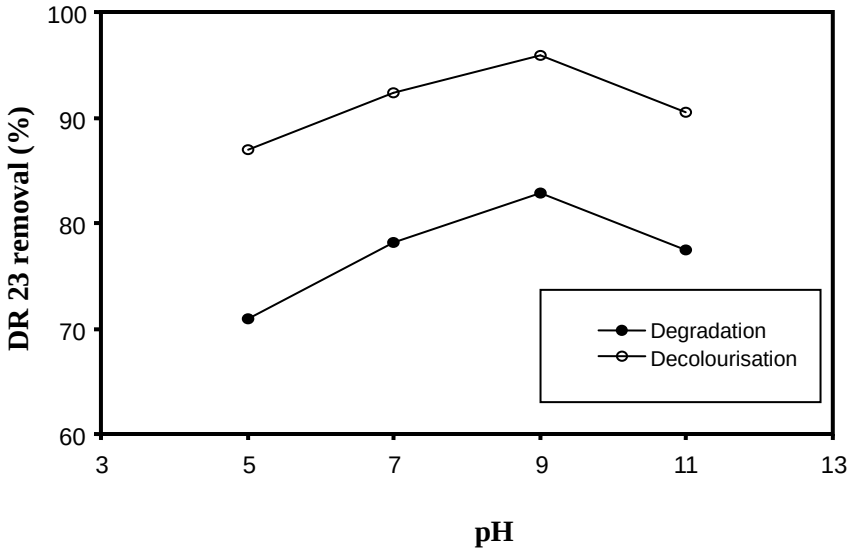

Figure 4. Effect of initial pH on the decolourisation and degradation of DR 23 using Solar light. AC-ZnO = 4 g/L, [DR 23] = 2×10^{-4} mol/L, irradiation time decolourisation = 60 minutes, degradation = 60 minutes.

3.3.2. Effect of solution pH

The effect of initial pH on the photodecolourisation and degradation efficiency of DR 23 was examined in the range of 5-11 in an aqueous suspension (Fig. 4). The results showed a sharp increase in degradation efficiency from pH 5 to 9. At pH 9 the maximum percentage removal of DR 23 was achieved and above pH 9 the removal efficiency decreased. It is well established that photodegradation depends upon the adsorption of the dye on the surface of the catalyst. The adsorption of the dye is greatly influenced by pH of the solution used [26-28]. Adsorption experiments carried out in dark showed maximum adsorption at pH 9. This is the reason for maximum efficiency at pH 9. Above pH 9, degradation efficiency decreases due to reduced adsorption.

3.3.3. Effect of grinding

To find out the effect of grinding on adsorption and degradation an intimate mixture of AC and ZnO was obtained by grinding them in a mortar with the required ratio. Kinetic curves for decolorisation and degradation by ZnO, Ground AC-ZnO and pepared AC-ZnO are displayed in Figures 5a and 5b respectively.

Grinding had practically negative effect both on adsorption and on the rates of decolourisation and degradation of DR 23. As shown by slopes the rate is higher for prepared AC-ZnO than Ground AC-ZnO.The amount of dye adsorbed in dark at 30 min on the ground 9AC-ZnO (30.0%) is slightly less than the dye adsorbed on prepared 9AC-ZnO (33.0%). Grinding can slightly oxidize the surface of AC thus increasing its surface acidity [22] and thereby decreasing DR 23 adsorption. In addition grinding may produce some crystal defects in the lattice of ZnO which behave as electron-hole recombination centers reducing photocatalytic activity.

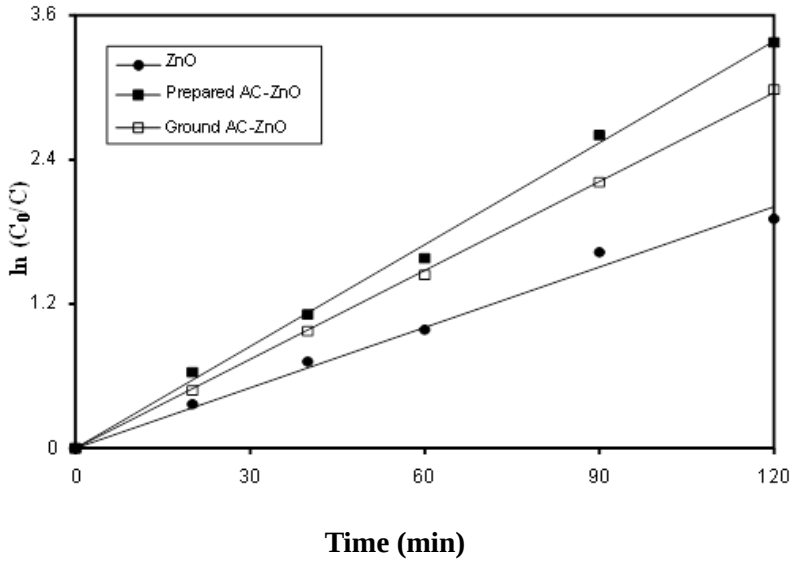

Figure 5a. Kinetics of DR 23 decolourisation for prepared and ground AC-ZnO catalysts using Solar light. AC-ZnO = 4 g/L, [DR 23] = 2×10^{-4} mol/L, pH = 7.0 ± 0.1

3.3.4. Effect of initial dye concentration

It is important both from mechanistic and application point of view to study the dependence of the photocatalytic reaction rate on the substrate concentration. The effect of initial dye concentration on the decolourisation and degradation efficiency was investigated by varying the initial concentrations from 1 to 8 x 10^{-4} mol /L and the results are shown in Table 1.

Table 1. Effect of initial concentration of DR 23 on decolourisation and degradation rates.

$C_0(10^{-4})$ mol L^{-1}	Decolourisation			Degradation		
	k_{app} (10^{-2}) min^{-1}	$t_{1/2}$ min	r (10^{-5}) mol L^{-1} min^{-1}	k_{app} (10^{-2}) min^{-1}	$t_{1/2}$ min	r (10^{-6}) mol L^{-1} min^{-1}
1	13.27	5.22	0.47	6.35	10.91	3.46
2	4.98	13.92	0.63	2.74	25.29	5.17
4	3.16	21.93	1.16	1.96	35.36	7.07
6	1.75	39.60	1.26	0.72	96.30	5.33
8	1.46	47.47	1.38	0.55	126.00	6.00

k_{app} = apparent rate constant, $t_{1/2}$ = half life period, r = initial rate

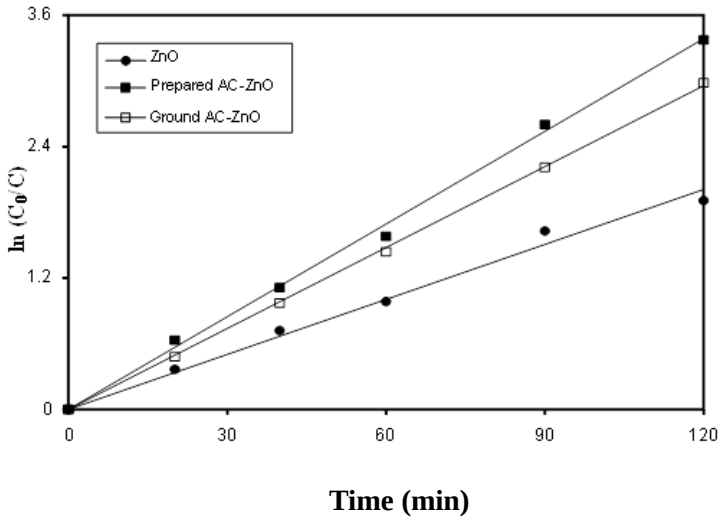

Figure 5b. Kinetics of DR 23 degradation for prepared and groundAC-ZnO catalysts using Solar light. AC-ZnO = 4 g/L, [DR 23] = 2 × 10^{-4} mol/L, pH = 7.0± 0.1.

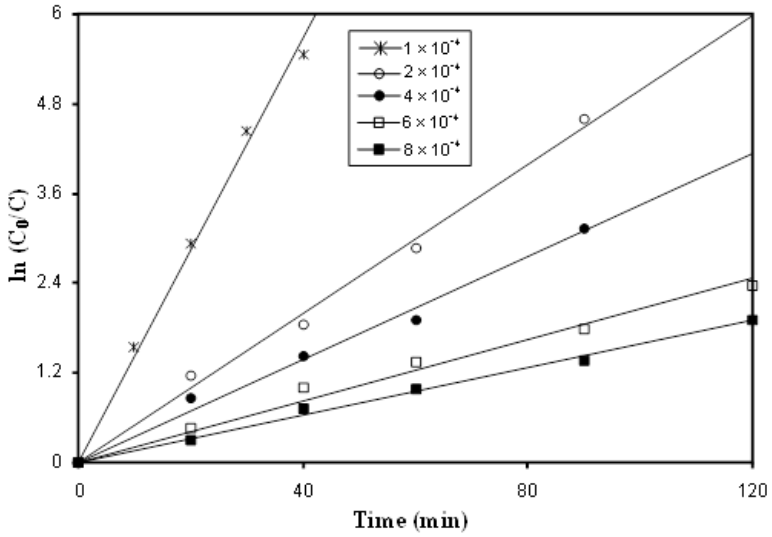

Figure 6. Kinetics of DR 23 decolourisation for different initial concentrations by Solar/AC-ZnO. AC-ZnO = 4 g/L, pH = 7.0 ± 0.1

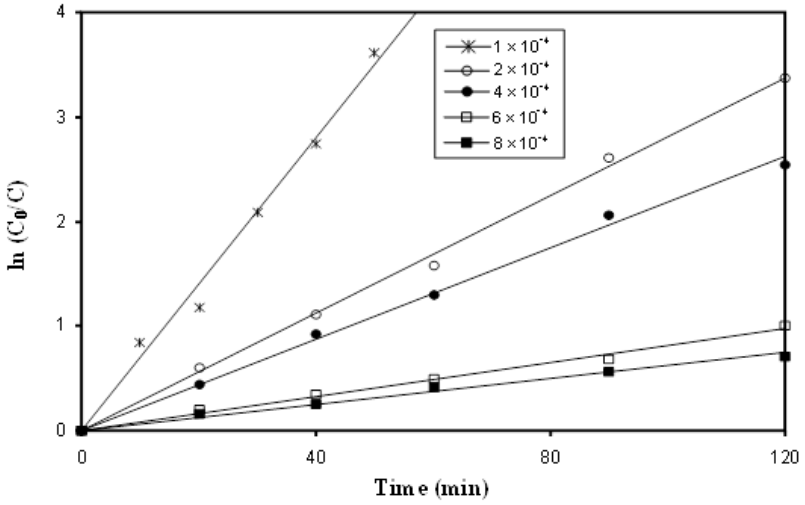

Figure 6b. Kinetics of DR 23 degradation for different initial concentrations by Solar/AC-ZnO. AC-ZnO = 4 g/L, pH = 7.0 ± 0.1

The results show that the degradation rate depends on the initial dye concentration. The rate constant *k* decreases with increase in the initial concentration of DR 23. Similar results have been reported for the photocatalytic oxidation of other dyes [29-31]. It is observed from the slopes of the lines in Figs. 6a and 6b that the degradation rate constant decreases rapidly at low DR 23 concentrations, and then changes slowly as the initial concentration increases.

The experimental data has been rationalized in terms of the modified form of L–H (Langmuir–Hinshelwood) kinetic model to describe the solid–liquid reaction successfully [24]. The rate of

degradation of DR 23 at the surface is proportional to the surface coverage of DR 23 on the ACSD-ZnO assuming that

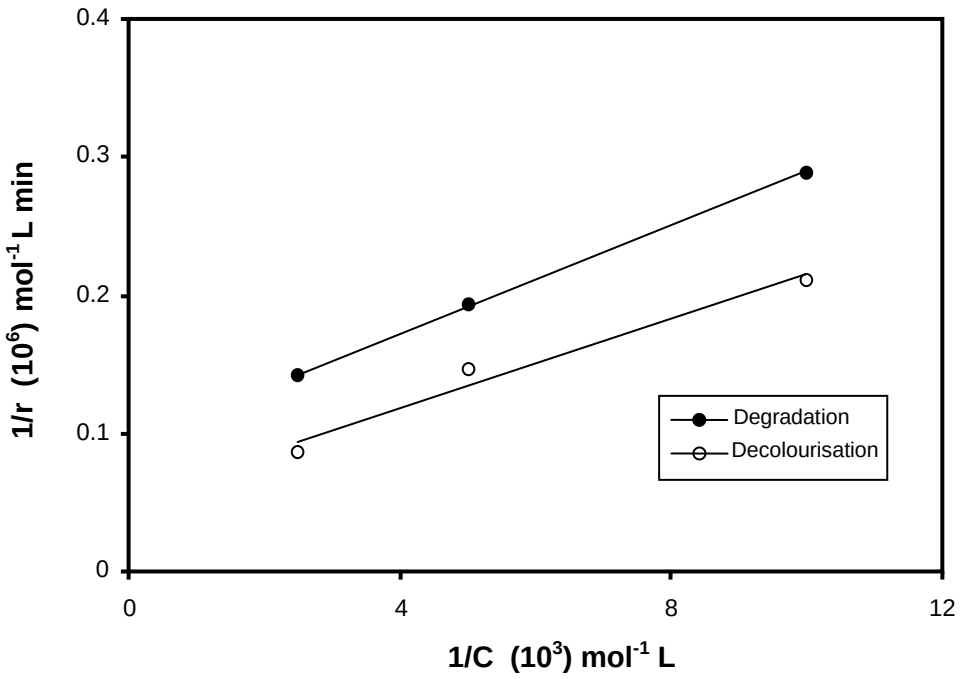

Figure 7. Linearised reciprocal kinetic plot of the decolourisation and degradation of DR 23 by Solar/AC-ZnO

the adsorption of DR 23 is more on the catalyst surface than the intermediate products. The effect of the DR 23 concentration on the rate of degradation is given in the following equation.

$$r = \frac{Kkc}{1+KC}$$

This equation can be modified as

$$\frac{1}{r} = \frac{1}{kKc} + \frac{1}{k}$$

where C is the initial concentration of DR 23, k is the reaction rate constant and K is the Langmuir adsorption constant. The reaction rate constant, k, reflects the limiting rate of the reaction at maximum coverage under the given experimental conditions and K represents the equilibrium constant for adsorption of DR 23 on the illuminated ACSD-ZnO.

At lower concentrations of the dye, the applicability of L-H equation for the decolourisation and degradation of DR 23 using solar light has been confirmed by the linear plot obtained by plotting the reciprocal of initial rate (1/r) against reciprocal of initial concentration (1/C) (Fig. 7).

The values *k* and K are found to be 1.85×10^{-5} Mm^{-1} and 3.37×10^{3} M^{-1} for decolourisation and 1.07×10^{-5} Mm^{-1}, 4.79×10^{3} M^{-1} for degradation respectively.

4. CONCLUSIONS

This study shows the efficiency of Activated carbon loaded ZnO, on the photodegradation of DR 23 and can be used as an inexpensive and highly effective alternative catalyst for the removal of environmental pollutants. Higher efficiency of AC-ZnO is due to its synergetic effect and its synergistic factor is 1.78. The optimum pH and the catalyst concentration for efficient removal of dye are found to be 9 and 4 g L^{-1}, respectively. Kinetic analysis of degradation reveals that the degradation follows pseudo-first order kinetics.The increase of initial dye concentration decreases the degradation rate. Therefore, the as-synthesized Activated carbon (ACSD) loaded ZnO can be used as an economical and environmentally friendly photocatalytic material in pollution control applications.

REFERENCES

[1] Muruganandham, M.; Suri, R. P. S.; Jafari, Sh.; Sillanpaa, M.; Lee, G. J.; Wu, J. J.; Swaminathan, M. Recent Developments in Homogeneous Advanced Oxidation Processes for Water and Wastewater Treatment, *Int. J. Photoenergy* **2014** (*2014*) 21Pages.

[2] Muruganandham, M.; Suri, R. P. S.; Sillanpaa, M.; Wu, J. J.; Ahmmad, B.; Balachandran, S.; Swaminathan, M. Recent Developments in Heterogeneous Catalyzed Environmental Remediation Processes *J. Nanosci. Nanotechnol.* **2014**, *4*, 1898-1910.

[3] Muthuvel, I.; Swaminathan, M. Highly solar active Fe(III)-immobilised alumina for the degradation of Active Violet 7, *Sol. Energy Mater. Sol. Cells* **2008**, *92*, 857-863.

[4] Zeng, H. B.; Cai, W. P.; Liu, P. S.; Xu, X. X.; Zhou, H. J.; Klingshirn, C.; Kalt, H. ZnO-based hollow nanoparticles by selective etching: elimination and reconstruction of metal-semiconductor interface, improvement of blue emission and photocatalysis. *Acs Nano*, **2008**, *2*, 1661-1670.

[5] Zhang, H.; Wu, J. B.; Zhai, C. X.; Du, N.; Ma, X. Y.; Yang, D.R. From ZnO nanorods to 3D hollow microhemispheres: solvothermal synthesis, photoluminescence and gas sensor properties, *Nanotechnol*, **2007**, *18*, 455604.

[6] Hu, X.; Gong, J.; Zhang, L.; Yu, J. C. Continuous Size Tuning of Monodisperse ZnO Colloidal Nanocrystal Clusters by a Microwave-Polyol Process and Their Application for Humidity Sensing, *Adv. Mater.* **2008**, *20*, 4845-4850.

[7] Shen, G. Z.; Bando, Y.; Liu, B.; Golberg, D.; Lee, C. Characterization and Field-Emission Properties of Vertically Aligned ZnO Nanonails and Nanopencils Fabricated by a Modified Thermal-Evaporation Process, *Adv. Funct. Mater.* **2006**, *16* , 410-416.

[8] Wang, Z. Y.; Huang, B. B.; Qin, X. Y.; Zhang, X. Y.; Wang, P.;, Wei, J. Y.; Zhan,J.; Jing, X. Y.; Liu, H. X.; Xu, Z. H.; Cheng, H. F.; Wang, X. N.; Zheng, Z. K. Growth of high transmittance vertical aligned ZnO nanorod arrays with polyvinyl alcohol by hydrothermal method, *Mater. Lett.* **2009**, 63, 130-132.

[9] Ueda, K.; Tabata, H.; Kawai, T. Magnetic and electric properties of transition-metal-doped ZnO films, *Appl. Phys. Lett.***2001**,*79*, 988-990.

[10] Wang, Z. L.; Song, J. H. Piezoelectric Nanogenerators Based on Zinc Oxide Nanowire Arrays, *Science*,**2006**, *312*, 242-246.

[11] Pozzo, R. L.; Baltanas, M. A.; Cassano, A. E. Supported titanium oxide as photocatalyst in water decontamination: State of the art, *Catal. Today*, **1997**,39, 219-231.

[12] Zhou Z, Yu J & Cheng B, Effects of Fe-doping on the photocatalytic activity of mesoporous TiO_2powders prepared by an ultrasonic method. *J. Hazard. Mater. B* **2006**,*137*, 1838-1842.

[13] Klingshirn, C. ZnO: material, physics and applications, *Chem. Phys. Chem.* **2007**, *8* 782-803.

[14] Mohameda, R. M.; Aazama, E. S. Enhancement of photocatalytic activity of ZnO–SiO_2 by nano-sized Ag for visible photocatalytic reduction of Hg(II), *Desalination Water Treat.* **2012**, *50*,140-146.

[15] Tsumura, T.; Kojitani, N.; Izumi, I.; Iwashita, N.; Toyoda, M.; Inagaki, M. Carbon coating of anatase-type TiO_2 and photoactivity, *J. Mat. Chem.* **2002**, *12 (5)*,1391-1396.

[16] Xu, Y.; Zheng, W.; Liu, W. Enhanced photocatalytic activity of supported TiO_2: dispersing effect of SiO_2, J. *Photochem. Photobiol. A: Chem.* **1999**,*122*, 57-60.

[17] Shimizu, K.; Kaneko, T.; Fujishima, T.; Kodama, T.; Yosida, H.; Kitayama, Y. Selective oxidation of liquid hydrocarbons over photoirradiated TiO_2 pillared clays, *Appl. Catal. A: Gen.* **2002**, *225*, 185-191.

[18] Matos, J.; Laine, J.; Herrmann, J. M. Effect of the Type of Activated Carbons on the Photocatalytic Degradation of Aqueous Organic Pollutants by UV-Irradiated Titania, *J. Catal.* **2001**,*200*, 10-20.

[19] Arana, J.; Dona Rodriguez, J. M.; Garriga i Cabo, C.; Gonzalez- Diaz, O.; Herrera-Melian, J. A.; Perez Pena, J.; Colon, G.; Navio, J. A. TiO_2 activation by using activated carbon as a support: Part I. Surface characterisation and decantability study, *Appl. Catal. B: Environ.* **2003**,*44*, 161-172.

[20] Pulido Melian, E.; Gonzalez Diaz, O.; Dona Rodriguez, J. M.; Colon, G.; Arana, J.; Herrera Melian, J.; Navio, J. A.; Perez Pena, J. ZnO activation by using activated carbon as a support: Characterisation and photoreactivity, *Appl. Catal. A Gen.* **2009**,*364*,174-181.

[21] Muthirulan, P.; Meenakshisundararam, M.; Kannan, N. Beneficial role of ZnO photocatalyst supported with porous activated carbon for the mineralization of alizarin cyanin green dye in aqueous solution, *J. Adv. Res*. **2013**, *4*, 479-484.

[22] Sobana, N.; Swaminathan, M. Combination effect of ZnO and activated carbon for solar assisted photocatalytic degradation of Direct Blue 53, *Solar Eng. Mater. Solar Cells*, **2007**, *91*,727-734.

[23] Sobana, N.; Muruganandham, M.; Swaminathan, M. Characterization of AC-ZnO catalyst and its photocatalytic activity on 4-acetylphenol degradation, *Catal. Commun.* **2008**, *9*,262-268.

[24] Sobana, N.; Krishnakumar, B.; Swaminathan, M. Synergism and effect of operational parameters on solar photocatalytic degradation of an azo dye Direct Yellow 4) using activated carbon-loaded zinc oxide, *Mater. Sci. Semiconduc. Process.* **2013**, *16*, 1046-1051.

[25] Balachandran, S.; Prakash, N.; Thirumalai, K.; Muruganandham, M.; Sillanpa, M.; Swaminathan, M. Facile Construction of Heterostructured BiVO4−ZnO and Its Dual Application of Greater Solar Photocatalytic Activity and Self-Cleaning Property, *Ind. Eng. Chem. Res.***2014**, *53*, 8346-8356.

[26] Balachandran, S.; Thirumalai, K.; Swaminathan, M. Facile hydrothermal synthesis of a highly efficient solar active Pr6O11–ZnO photocatalyst and its multiple applications ,*RSC Adv.*, **2014**,*4*, 27642-27653.

[27] Velmurugan, R.; Swaminathan, M. An efficient nanostructured ZnO for dye sensitized degradation of Reactive Red 120 dye under solar light *Sol. Energy Mater. Sol.Cells,* **2011**, *95*, 942-950.

[28] Balachandran, S.; Swaminathan, M. Facile Fabrication of Heterostructured Bi_2O_3–ZnO Photocatalyst and Its Enhanced Photocatalytic Activity, *J. Phys. Chem. C* **2012**, 116, 26306-26312.

[29] Matos, J.; Laline, J.; Herrmann, J. M. Synergy effect in the photocatalytic degradation of phenol on a suspended mixture of titania and activated carbon, *Appl. Catal. B* **1998**,*18*, 281-291.

[30] Neppolian, B.; Choi, H. C.; Sakthivel, S.; Arabindoo, B.; Murugesan, V. Solar/UV-induced photocatalytic degradation of three commercial textile dyes, *J. Hazard Mat. B.* **2002**, *89*, 303-317.

[31] Yatmaz, H.C.; Akyol, A.; Bayramoglu, M. Kinetics of the photocatalytic decolorization of an azo reactive dye in aqueous ZnO suspensions, *Ind. Eng. Chem. Res.***2004**, *43*, 6035-6039.

The authors declare no conflict of interest

© 2016 By the Authors; Licensee Borderless Science Publishing, Canada. This is an open access article distributed under the terms and conditions of the Creative Commons Attribution license http://creativecommons.org/licenses/by/3.0